

Design of a High Speed Claw Pole Motor with Soft Magnetic Composite Core

Yunkai Huang^{1,2}, Jianguo Zhu², Youguang Guo² and Qiansheng Hu¹

¹School of Electrical Engineering, Southeast University, China

²Faculty of Engineering, University of Technology, Sydney, Australia

Soft magnetic composite (SMC) materials are particularly suitable for application in electrical machines with complex structures, 3D magnetic flux paths, and high operating frequencies, because of their unique properties. This paper presents the design of a 2 kW high speed (30 krpm) three stack claw pole motor with SMC core. Three-dimensional finite element analysis of magnetic field is conducted for parameter calculation and dimension optimisation. Considering the importance of core loss for the design of high speed motors, rotational core loss model is employed in this paper. Practical methods considering the alternating magnetic field only are also presented, which are useful to designers who do not have rotational core loss data.

Key Words: High speed motor, Claw pole motor, Soft magnetic composite, Finite element analysis, Core loss.

1. Introduction

High speed motors have been employed in many applications, such as machine tool spindles, aerospace, centrifugal compressors, vacuum pumps, friction welding units, turbine generators, and etc. Compared with conventional general-purpose motors, the major advantages of high speed motors include smaller size under given power, higher power and torque density, smaller moment of inertia and fast response, and direct connection with other high speed mechanical devices without gear.

Induction motors [1], [2], switched reluctance motors [3], and permanent magnet motors [4], [5] are suitable for high-speed operation, especially when variable speed is required. It is difficult to identify the "best", as the motor performance is not the only concern. Controller, control strategy, whole system efficiency, manufacturability, cost and commercialization potential should also be considered. Table 1 tabulates the advantages and disadvantages of each type of motor for high speed operation.

Soft magnetic composite (SMC) materials are very suitable for application in permanent magnet motors with complex structures, 3D magnetic flux paths, and high operating frequencies, because of their unique properties such as magnetic and thermal isotropy, low eddy current loss, and suitability for complex net shape manufacturing by highly matured powder metallurgical technology [6].

Correspondence: Yunkai Huang, School of Electrical Engineering, Southeast University, Sipailou 2#, Nanjing 210096, China, email: huangyunkai@gmail.com

Fig. 1 plots the core losses of SOMALOYTM 500 (an SMC material) and various commonly used SiFe sheets under alternating excitation at 1.0 T versus frequency. Because of low eddy current, the core loss of SMC starts to become lower than that of SiFe when the frequency reaches about 700 Hz.

Table 1. Advantages and disadvantages of electrical machines for high speed operation

Machine Type	Advantages	Disadvantages
Induction Motor	Easy starting Easy for fabrication Low cost No position sensor	Small air gap length Low power factor Rotor loss in high frequency
Permanent magnet motor	Large air gap length High power factor Various structure	Rotor robustness Need position sensor Field weakening for super high-speed
Switched reluctance motor	Simple rotor structure Low rotor loss	Small air gap length Low power factor Windage loss Need position sensor Noise

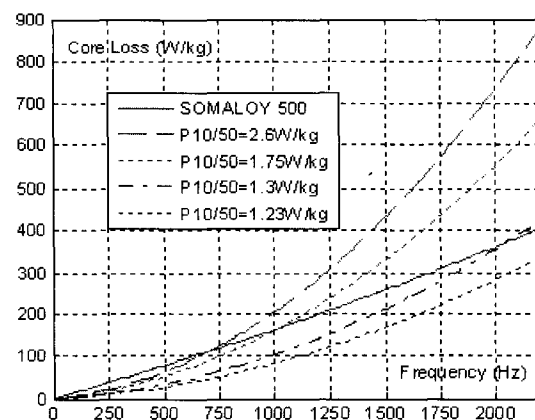


Fig. 1. Core losses of SMC and SiFe versus frequency

The operational frequency of high speed motors is normally over 1000 Hz, and even 5000 Hz for super-high speed motors, so SMC is an ideal candidate as the core. This paper presents the investigation on a 3-phase 3-stack permanent magnet (PM) claw pole motor with SMC core.

2. Number of Poles

The pole number affects the motor structure and performance. When the number of poles increases, the core loss becomes larger due to the increased operational frequency if the rotor speed remains the same. Because the eddy current loss of SMC material is very low, the total core loss is almost directly proportional to the frequency, as shown in Fig. 2. However, the amount increased also depends on the core material and magnetic flux density.

The copper loss will decrease when the pole number is increased. Fig. 3 illustrates the core loss and copper loss versus pole number when the overall motor size is kept the same. It is noted that the increase of core loss is minor. When the number of poles increases, the average magnetic density in the stator core (particularly the yoke) decreases because the flux per pole is reduced. To avoid excessive switching losses in the power electronic components, the number of poles is chosen as 4 with an operating frequency of 1 kHz finally.

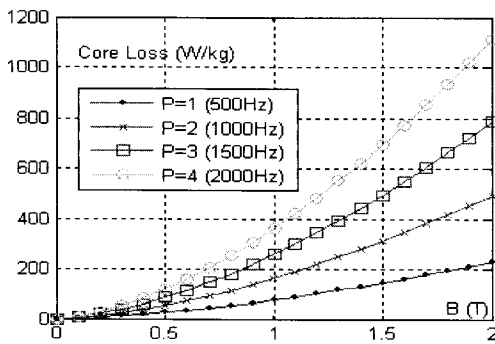


Fig. 2. Core loss vs frequency (P: number of pole-pairs)

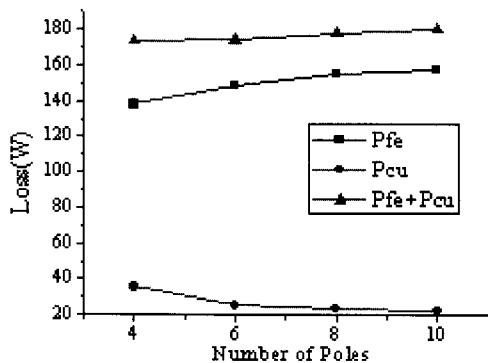


Fig. 3. Core loss and copper loss versus pole number when the motor overall size keeps the same

3. 3D Magnetic Field FEA

The claw pole motor has a structure of 3D flux, therefore 3D magnetic field finite element analysis (FEA) is desired for accurate calculation of motor parameters and performance. In this paper, the commercial software ANSYS was used. Taking advantage of the periodical symmetry, only one pole pitch region of one stack, as shown in Fig. 4, needs to be calculated. The magnetic coupling between stacks is negligible.

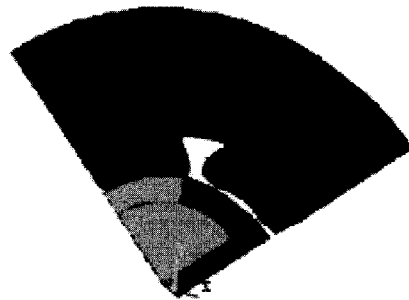


Fig. 4. Region for field solution

At the two radial boundary planes, the magnetic scalar potential obeys the half-periodical boundary conditions [6]:

$$\varphi_m(r, \Delta\theta/2, z) = -\varphi_m(r, -\Delta\theta/2, -z) \quad (1)$$

where $\Delta\theta=90^\circ$ is the mechanical angle of one pole pitch. The major path of the magnetic flux is along the north pole of the PM → air gap → one claw pole → stator yoke → another claw pole → air gap → south pole of the PM → rotor yoke to form a closed loop. The winding flux can be computed by the surface integral of magnetic density after the magnetic field distribution is solved by FEA. For this motor, the computation is based on the middle cross-sectional area of the stator yoke. There is also a considerable amount of leakage flux closing through the air between the adjacent claw poles.

3.1 Dimensional parameters

Fig. 5 shows the dimensional parameters, which are determined and optimized by FEA to achieve the maximum winding flux.

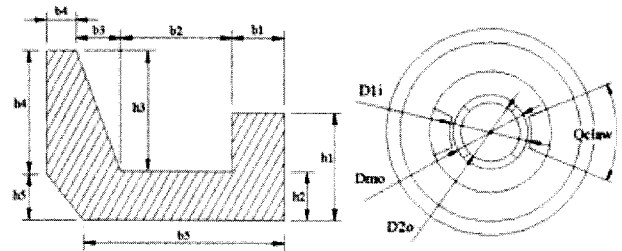


Fig. 5. Dimensional parameters

3.2 Qclaw

When the claw pole arc, Q_{claw} , increases, the magnetic reluctance of magnetic circuit decreases and hence the winding flux may increase. However, if Q_{claw} is too big, the leakage flux between claw poles would become significant and the winding flux would decrease. Through calculation, as shown in Fig. 6, the winding flux (per turn) achieves the maximum value when Q_{claw} is about 75° .

3.3 b1, b2 and h2

The relations of the maximum winding flux versus dimensional parameters $b1$, $b2$ and $h2$ are investigated. Fig. 7 shows the variation of the maximum winding flux against the stator yoke width, $b1$. $b2$ and $h2$ are the dimensions which determine the coil space and the copper fill factor is $S_f = S_{coil} / (b2 * 2 * (h1 - h2))$. Table 2 lists possible combinations of $b2$ and $h2$ when the copper fill factor is kept the same.

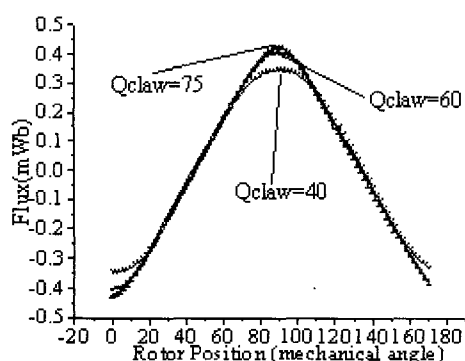


Fig. 6. Winding flux waveform in different Q_{claw}

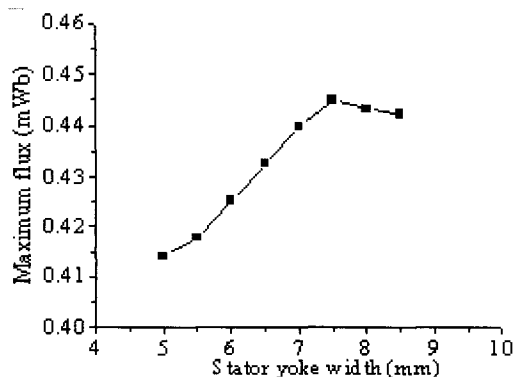


Fig. 7. Maximum flux versus stator yoke width

Table 2. Different combinations of $b2$ and $h2$

$b2$ (mm)	$h2$ (mm)	Maximum flux (mWb)
6.5	6.1	0.4286
6.8	6.4	0.4290
7	6.6	0.4294
7.2	6.8	0.4288
7.5	7	0.4252
8	7.4	0.4245

The final dimensions are: $b1=7.5$ mm, $b2=7$ mm, $b3=3$ mm, $b4=2$ mm, $h1=13$ mm, $h2=6.6$ mm, $h3=16.4$ mm, $h4=20$ mm, $h5=3$ mm, $Q_{claw}=75^\circ$, $D2o=20$ mm, $Dmo=26$ mm, and $D1i=28$ mm.

4. Core Loss

In a high speed motor, the calculation of core loss is crucial for performance analysis because the core loss is the dominant component of power loss. However, the core loss calculation can be very complex as the magnetic density distribution in a claw pole motor is much more complicated than that in a conventional laminated PM motor.

4.1 Rotational model

The core loss is caused not only by alternating but also by rotational magnetic fields, and should be considered properly in the motor design [7]. An improved model described in [7], [8] is applied for predicting the core loss in the 3D-flux SMC motor. Different formulations for alternating and rotational magnetic field are summarized in the follows:

If the magnetic density is sinusoidal (e.g. the fundamental component), the alternating core loss is calculated by:

$$P_{al} = K_{ha} f B_m^h + K_{ea} (f B_m)^2 + K_{aa} (f B_m)^{1.5} \quad (\text{W/kg}) \quad (2)$$

and the core loss with circular magnetic density by

$$P_r = P_{hr} + K_{er} (f B_m)^2 + K_{ar} (f B_m)^{1.5} \quad (\text{W/kg}) \quad (3)$$

where

$$\frac{P_{hr}}{f} = a_1 \left[\frac{1/s}{(a_2 + 1/s)^2 + a_3^2} - \frac{1/(2-s)}{[a_2 + 1/(2-s)]^2 + a_3^2} \right]$$

$$s = 1 - \frac{B_m}{B_s} \sqrt{1 - \frac{1}{a_2^2 + a_3^2}} \quad (4)$$

The coefficients K_{ha} , h , K_{ea} , K_{aa} , K_{er} , K_{ar} , a_1 , a_2 , a_3 and B_s can be deduced from the data measured by the 2D [9] and 3D [10] rotational core loss tester. B_m is the peak value of sinusoidal flux density.

The core loss with elliptical B is predicted from the alternating and circularly rotating core losses by:

$$P_{fe} = R_B P_r + (1 - R_B)^2 P_{al} \quad (5)$$

where $R_B = B_{min} / B_{maj}$ is the axis ratio, B_{maj} and B_{min} are the major and minor axes of the elliptical B locus.

The core loss is computed based on time-stepping FEA. One electrical period is divided into 18 steps. The meshing of stator and rotor is kept the same in each step. Core loss in each element is calculated, and then the total core loss of the motor is obtained by summing up the losses of all the elements.

4.2 Alternating method

Rotational model is an accurate method to predict the core loss, but the corresponding data are difficult to acquire. Two practical methods considering only the alternating magnetic field are presented and compared with the rotational model.

4.2.1 Waveform method

The magnetic flux density B is decomposed to radial, circumferential and axial components, *i.e.* B_r , B_θ and B_z . The waveform of each component versus rotor position is obtained through the time-stepping FEA. Each component is expanded into Fourier series, and the core loss in each element can be expressed as:

$$P_{fe_i} = \sum_{k=1}^{\infty} (K_{ha} k f B_{ikm}^h + K_{ea} (k f B_{ikm})^2 + K_{aa} (k f B_{ikm})^{1.5}) \quad (6)$$

where $i=r, \theta, z$, and B_{ikm} is the peak value of the k -th harmonic flux density.

4.2.2 Locus method

The locus of each element is computed as stated in Section 4.1. The core loss in an element can be expressed as:

$$P_{fe} = K_{ha} f B_{maj}^h + K_{ea} (f B_{maj})^2 + K_{aa} (f B_{maj})^{1.5} + K_{ha} f B_{min}^h + K_{ea} (f B_{min})^2 + K_{aa} (f B_{min})^{1.5} \quad (7)$$

4.3 Comparison

The results calculated by the three methods are shown in Fig. 8. The locus method is more accurate than the waveform method.

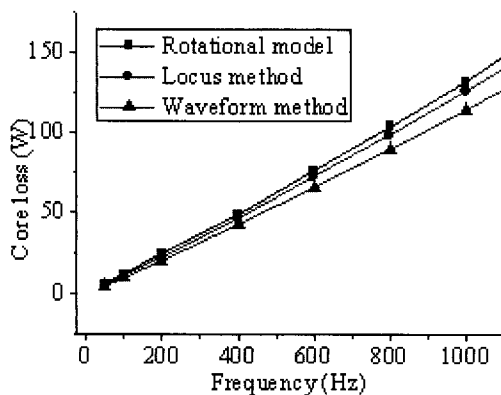


Fig. 8. Comparison of core losses by different models

5. Conclusion

Due to the very low eddy current loss, SMC material is suitable for high speed motor. This paper

presents the design and analysis of a high speed 3-phase 3-stack permanent magnet claw pole motor with SMC core. 3D FEA magnetic field analysis is employed for optimizing the dimensions to acquire the maximum winding flux and calculating the core loss. The locus method considering only alternating field is useful to the designers who do not have rotational core loss data.

References

- [1] M. Johansson, M. Larsson, L. Naslund and J. Hylander, "Small high-speed induction motors," *Proc. IEEE Int. Electric Machines and Drives Conf.*, pp. 279-284, 2003.
- [2] W. L. Soong, G. B. Kliman, R. N. Johnson, R. A. White and J. E. Miller, "Novel high-speed induction motor for a commercial centrifugal compressor," *IEEE Trans. Industry Applications*, Vol. 36, No. 3, pp. 706-713, 2000.
- [3] L. Morel, H. Fayard, H. Vives Fos, A. Galindo and G. Abba, "Study of ultra high speed switched reluctance motor drive," *Conf. Record of 35th IEEE Industry Applications Society Annual Meeting*, pp. 87-92, 2000.
- [4] A. Binder, T. Schneider and M. Klohr, "Fixation of buried and surface mounted magnets in high-speed permanent magnet synchronous motors," *Conf. Record of 40th IEEE Industry Applications Society Annual Meeting*, Hong Kong, China, pp. 2843-2848, 2000.
- [5] N. Bianchi, S. Bolognani and F. Luise, "Analysis and design of a PM brushless motor for high-speed operations," *IEEE Trans. Energy Conversion*, Vol. 20, No. 3, pp. 629-637, 2005.
- [6] Y. G. Guo, J. G. Zhu, P. A. Watterson and W. Wu, "Comparative study of 3-D flux electrical machines with soft magnetic composite core," *IEEE Trans. Ind. Application*, Vol. 39, pp. 1696-1703, 2003.
- [7] J. G. Zhu and V. S. Ramsden, "Improved formulations for rotational core losses in rotating electrical machines," *IEEE Trans. Magn.*, Vol. 34, pp. 2234-2242, 1998.
- [8] Y. G. Guo, J. G. Zhu, J. J. Zhong and W. Wu, "Core losses in claw pole permanent magnet machines with soft magnetic composite stators," *IEEE Trans. Magn.*, Vol. 39, pp. 3199-3201, 2003.
- [9] J. G. Zhu, J. J. Zhong, V. S. Ramsden and Y. G. Guo, "Power losses of composite soft magnetic materials under two dimensional excitations," *Journal of Applied Physics*, Vol. 85, pp. 4403-4405, 1999.
- [10] Y. G. Guo, J. G. Zhu, Z. W. Lin and J. J. Zhong, "Measurement and modeling of core losses of soft magnetic composites under 3-D magnetic excitations in rotating motors," *IEEE Trans. Magn.*, Vol. 41, No. 10, pp. 3925-3927, 2005.

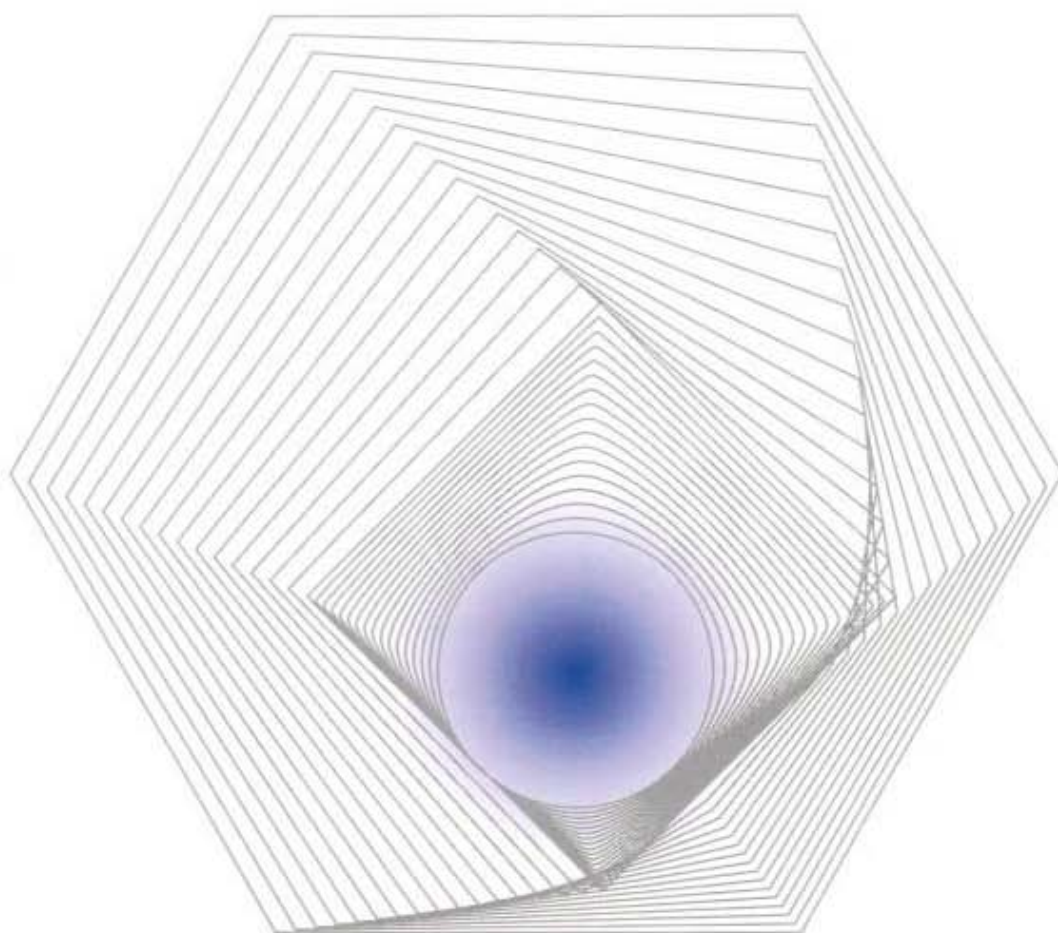
Received: 20 July 2006/Revised: 31 January 2007



AEM

Journal of the Japan Society of Applied
Electromagnetics and Mechanics

 日本AEM学会誌



Asia-Pacific Symposium on Applied Electromagnetics and Mechanics 2006 (APSAEM06)

Volume **15** Supplement September 2007